J. Plasma Fusion Res. SERIES, Vol. 2 (1999) 255–258

Simulation Study of Energetic Particle Distributions during ICRF and NBI Heating in the LHD Plasma

MURAKAMI Sadayoshi, NAKAJIMA Noriyoshi and OKAMOTO Masao
National Institute for Fusion Science, Toki 509-5292, Japan

(Received: 26 January 1999 / Accepted: 20 May 1999)

Abstract

Energetic particle distributions during ICRF and NBI heating are studied numerically including complex motions of energetic particles in LHD. Linearized drift kinetic equation in a three dimensional magnetic field is solved based on the Monte Carlo techniques and the steady state solutions are obtained. Characteristics of the energetic particle distributions for ICRF and NBI heating are clarified in the LHD plasma.

Keywords:
energetic particle, ICRF heating, NBI heating, LHD, Monte Carlo simulation

1. Introduction

Plasma heating generally produces energetic particles at first (e.g. beam injection, RF wave acceleration) and, then, the energy of these particle transfer to the bulk plasma through particle collisions. In this process the behaviour of energetic particles plays important roles. The radial diffusion of energetic particles enhances the broadening of heating profiles and the orbit loss of energetic particles reduces the heating efficiency. Additionally, the energetic particles by plasma heating could cause the anisotropic pressure profile and inhomogeneous pressure profile on magnetic surfaces due to trapped particle effect, and these would affect on the confinement of the bulk plasma. Thus the analysis of energetic particle distribution is necessary for understanding of the plasma heating and energetic particle effects on the bulk plasma.

The studies of energetic particle distributions in tokamaks have been done by many authors, where the radial transport of energetic particles was ignored or treated by relatively simple orbit models. However, in non-axisymmetric configurations, trapped particle motions are complicated due to the three dimensional (3D) magnetic configuration and the orbit effect on the energetic particle distribution would be relatively large compared with that of tokamaks. Thus a different approach including complicated motions is necessary for studying the energetic particle distribution in non-axisymmetric configurations.

In this paper we study the energetic particle distribution for ICRF and NBI heating in the LHD plasma including complex motions of energetic particles. The linearized drift kinetic equations for energetic particles are solved in 5D phase space based on the Monte Carlo techniques.

2. Energetic Ion Distribution by ICRF Heating

High power ICRF heating is considered in LHD with the heating power more than 10MW and the frequency range from 25 to 95MHz. ICRF heating produces highly energetic trapped particles and these motions are very complicated in heliotrons. Therefore the confinement of energetic ions is an important issue for the ICRF heating in heliotrons. In previous papers

Corresponding author's e-mail: murakami@nifs.ac.jp

[1-3] we have shown the significant effect of energetic ion orbit loss on the heating efficiency. Thus the finite orbit effect would also be important in considering the energetic ion distribution in ICRF heating of LHD.

Here, we study the effect of complex drift motion on the energetic ion distribution by ICRF minority heating in the LHD plasma. We consider the linearized drift kinetic equation for minority ion distribution, f_{mi}, as

$$\frac{\partial f_{mi}}{\partial t} + v_D \cdot \nabla f_{mi} - C(f_{mi}) - L_{orbit}(f_{mi}) - S_{ptcl} = Q_{ICRF}(f_{mi}), \quad (1)$$

where $C(f_{mi})$ is the linear Coulomb Collision Operator [4], and Q_{ICRF}, S_{ptcl} and L_{orbit} are the ICRF heating term, particle source term and particle loss term by orbit loss, respectively. The time development of Eq. (1) is solved until the distribution becomes mostly steady state using the Monte Carlo simulation code [1,3]. In this simulation we assume that the particle source profile is same as that of bulk plasma density profile, $S = S_0\{1 - (r/a)^2\}$, and that the orbit loss boundary set to the outermost flux surface. The complex magnetic field configuration is also included using the Boozer coordinates based on 3D MHD equilibrium, where the equilibrium magnetic field is expressed by 33 poloidal and toroidal modes with 60 radial grid points.

Figure 1 shows the distribution of minority ions in the $(r, v_{\parallel}, v_{\perp})$ space in the standard configuration of the LHD [T_{e0} = 1.0keV, T_{i0} = 1.0keV, $n_0 = 1.0 \times 10^{20}$m^{-3}]. We can see that the euqi-contours of the velocity distribution function are elongated to the $v_{\perp}$ direction because of the perpendicular heating by ICRF heating. Also we find that the different shape of distributions at the central and outer regions. In the central region, the distribution is simply elongated Maxwellian distributions, however, the distribution in the outer region has a square shape. The helical ripple increases in the outer region and the helically trapped particle near the resonant region generates like this square shape distribution. Further in the edge regions the shape becomes inverted triangles due to the loss cone loss of energetic ions.

We, next, study the minority ion distribution in the real space. Figure 2 shows the cross-sectional view of effective pressure for minority ions, P_{mi} ($= \int E_{mi} f_{mi}\, dv$; E_{mi} is the total kinetic energy of a minority ion), at the toroidal angle where the magnetic surface is horizontally elongated. We can see the two peaks of P_{mi} at the central region (right hand side) and the outer region (left hand side). In this simulation the resonant magnetic field with an ICRF wave set to near the magnetic axis. Therefore the energetic ions are mainly generated near the axis and this explains the peak at the central region. On the other hand, the outer peak region corresponds to the minimum magnetic field point of helical ripple with resonant magnetic field strength. Since ICRF heated energetic ions move along the helical ripples keeping their magnetic field strength at the banana center, so it is considered that the outer peak is generated by the energetic trapped particles from the center region.

Consequently, it is found that the inhomogeneous pressure profile of the minority ions occurs on th flux surface in the ICRF heated LHD plasma. This non-uniform distribution could enhance other effects on bulk plasma and these are our future problems.

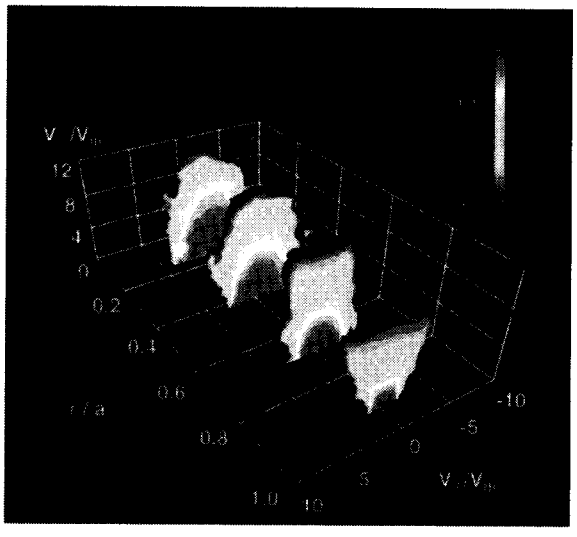

Fig. 1 Energetic ion distribution in the $(r, v_{//}, v_{\perp})$ space during the ICRF minority heating of LHD plasma. Plasma parameters are T_{e0} = 1keV, T_{i0} = 1keV, n_{e0} = 1.0×10^{20}m^{-3}.

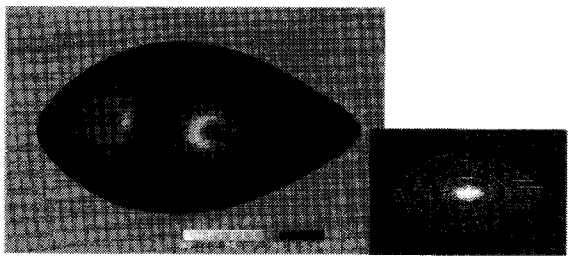

Fig. 2 Cross-sectional view of effective pressure for minority ions at the toroidal angle where magnetic surfaces are horizontally elongated.

3. Energetic Ion Distribution by NBI Heating

NBI heating system with tangential beam injection (P_{NBI} = 15MW and E_b =180keV) is considered in the LHD. Complex orbit effects due to trapped particle motions can be avoided for injected beam ions. However, the pitch angle scattering by collisions generates trapped energetic ions, which would affect the distribution of beam ions in LHD.

Using the same technique as that in Ref. 5, we evaluate the steady state distribution of NBI beam ions solving the linearized drift kinetic equation as

$$\boldsymbol{v}_D \cdot \nabla f_{beam} - C\left(f_{beam}\right) - L_{orbit}\left(f_{beam}\right) = S_{NBI}\,, \quad (2)$$

where $C(f_{beam})$ is the linear Coulomb Collision Operator. L_{orbit} is the particle loss term by orbit loss and the outermost flux surface is assumed as the orbit loss boundary in the simulation. And S_{NBI} is the beam particle source term evaluated by the NBI deposition code [6]. The same magnetic field model for the LHD configuration is used as that of ICRF heating case.

Figure 3 shows the obtained distribution of NBI beam ions in the (r, $v_{//}$, $v_\perp$) space in the standard configuration of LHD. We assume the characteristic plasma parameters obtained experimentally [7] as T_{e0} = 0.8keV, T_{i0} = 0.8keV, $n_0 = 0.4 \times 10^{20}$m^{-3}, and the beam ion energy to be 100keV. The highly energetic beam ions ($v_{//} \sim 15\ v_{th}$) are injected at the high $v_{//}$ region. Then, these energetic beam ions are slowed down to lower velocity. The pitch angle scattering starts when the beam ions reach to the critical velocity $v_c(\sim 4v_{the})$. We can see the slowing down distributions of beam ions due to the collisions with bulk plasma in the center region. The loss cone structure can be seen only near the edge region.

From obtained beam distribution we can evaluate the power deposition profile of NBI heating. In order to make clear the effect of trapped beam ions due to pitch angle scattering we compare the obtained deposition profile with the NBI data base results, in which the orbit effect due to pitch angle scattering is excluded. Figure 4 shows a comparison of NBI heating profiles with and without the trapped orbit effect. We can see a relatively good agreement between two deposition profiles. As a result we can conclude that the orbit effect is still small for the present plasma parameters.

4. Conclusions

We have studied the energetic particle distributions during ICRF and NBI heating in the LHD plasma including the effect of complex particle motions. The elongation of velocity distribution to the $v_\perp$ direction can be seen due to the ICRF heating and the loss cone structure in the distribution is observed near the edge region. The spatial distribution of energetic ions shows the two peaks of the effective pressure profile. This is because ICRF heated energetic ions move along the helical ripple. The loss cone structure has also found in the distribution of NBI beam particles near the edge region. The orbit effect during slow-down was found to

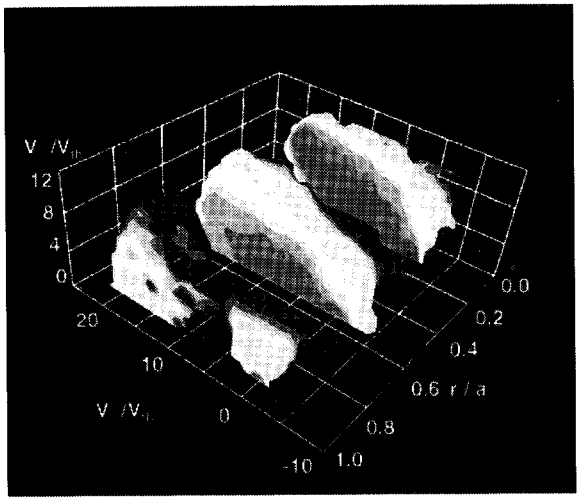

Fig. 3 Beam ion distribution in the (r, $v_{//}$, $v_\perp$) space during NBI heating of LHD plasma. The plasma parameters are T_{e0} = 0.8keV, T_{i0} = 0.8keV, n_{e0} = 0.4 × 10^{20}m^{-3}.

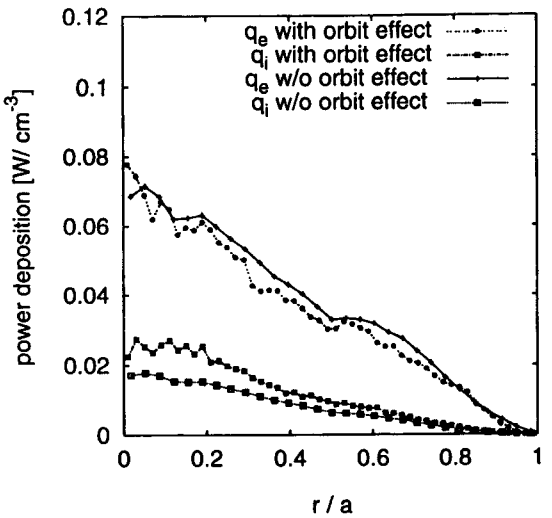

Fig. 4 Comparison of power deposition profiles with and without orbit effect during slow-down process.

be small for the present plasma parameters.

References

[1] S. Murakami *et al.*, Nucl. Fusion **34**, 913 (1994).

[2] S. Murakami *et al.*, *Plasma Phys. Controlled Nuclear Fusion Res.* 1994 (*Proc. 15th Int. Conf.* Seville, 1994), Vol. 3, IAEA, Vienna, 531 (1996).

[3] S. Murakami *et al.*, Fusion Eng. Design **26**, 209 (1995).

[4] Boozer and Kuo-Petravic, Phys. Fluids **24**, 851 (1981).

[5] S. Murakami *et al.*, *Proc. 17th IAEA Fusion Energy Conference* Yokohama 1998, IAEA, IAEA-CN-69/TH2/1.

[6] S. Murakami *et al.*, Trans. Fusion Technology **27**, 259 (1995).

[7] A. Iiyoshi *et al.*, *Proc. 17th IAEA Fusion Energy Conference* Yokohama 1998, IAEA, IAEA-CN-69/OV1/4.